Supplementary Information for

HIV-1 and microvesicles from T-cells share a common glycome, arguing for a common origin.

Lakshmi Krishnamoorthy[1], *Julian W. Bess, Jr.* [2], *Alex B. Preston*[1], *Kunio Nagashima*[3] *and Lara K. Mahal*[1*]

a

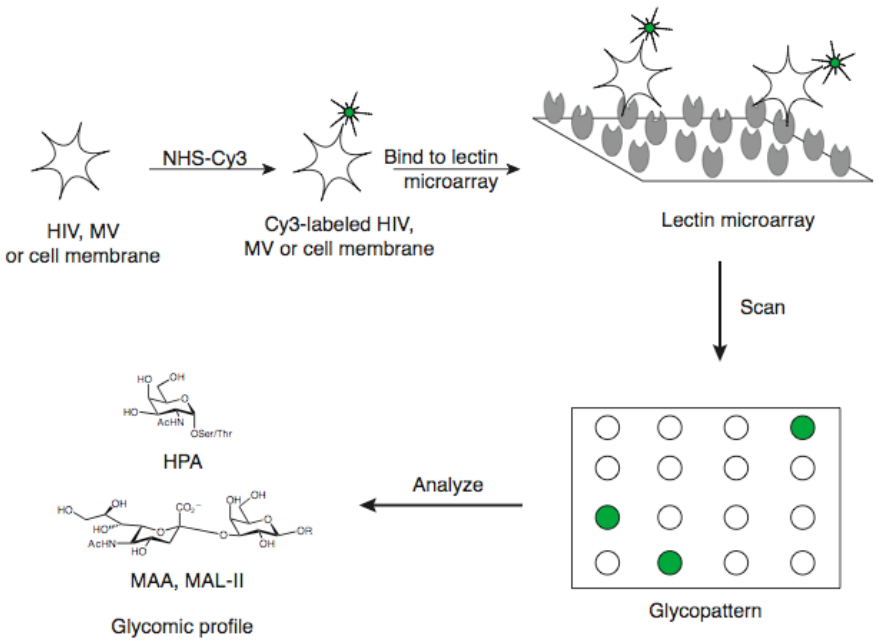
NHS-Cy3
Bind to lectin microarray
HIV, MV or cell membrane
Cy3-labeled HIV, MV or cell membrane
Lectin microarray
Scan
HPA
Analyze
MAA, MAL-II
Glycomic profile
Glycopattern

b

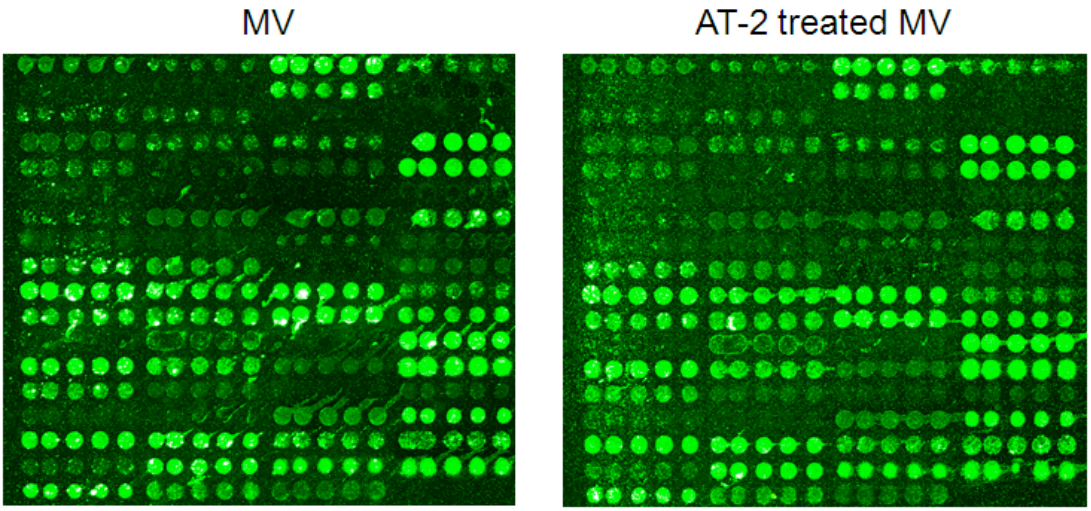
MV
AT-2 treated MV

c

APA	ABA	AAA	PNA
AIA	BPA	BDA	ConA
CCA	CAA	CPA	CA
CSA	DSA	DBA	ECA
EEA	GNA	SBA	GS-I
GS-II	HMA	HPA	IAA
LAA	LcH	LFA	Lotus
LEA	LPA	MAA	NPA
PAA	LBA	PHA-E	PHA-L
PSA	PSL	PTA	RPA
SNA	STA	SJA	TKA
RTA	WGA	TL	UEA-I
UEA-II	UDA	VGA	VVA
VVA(man)	VRA	VFA	WFA
Blackbean	RCA	HHL	AAL
MAA-I	MAA-II	PTL-I	PTL-II
CVN	SVN	GRFT	Gal-1

d

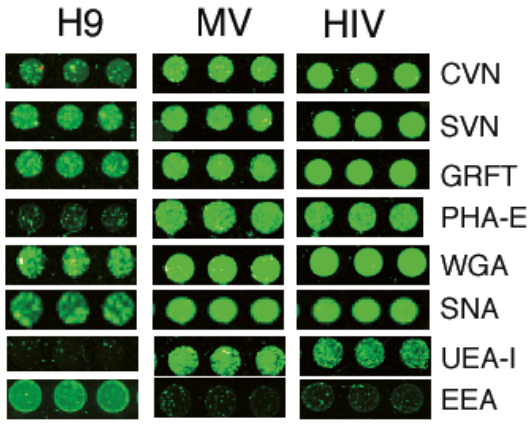

Supplementary Figure 1. Single color data for H9-derived microvesicles and HIV-1. (**a**) Schematic for a single color lectin microarray experiment. (**b**) Cy-3 labeled AT-2 treated and untreated H9-derived microvesicles (1 μg) were compared using the lectin microarray. Samples were from different lots of H9-derived microvesicles. Glycopatterns of the two samples are identical indicating that treatment with AT-2 does not significantly alter glycomic profiles. (**c**) Lectin print pattern for the arrays shown in **Fig. 1a** in the main text. For each lectin, 5 replicate spots are printed. Note, see **Supplementary Table 1** for the key to lectin abbreviations. (**d**) Direct comparison of a selected lectin subset from **Fig. 1a** is shown.

a

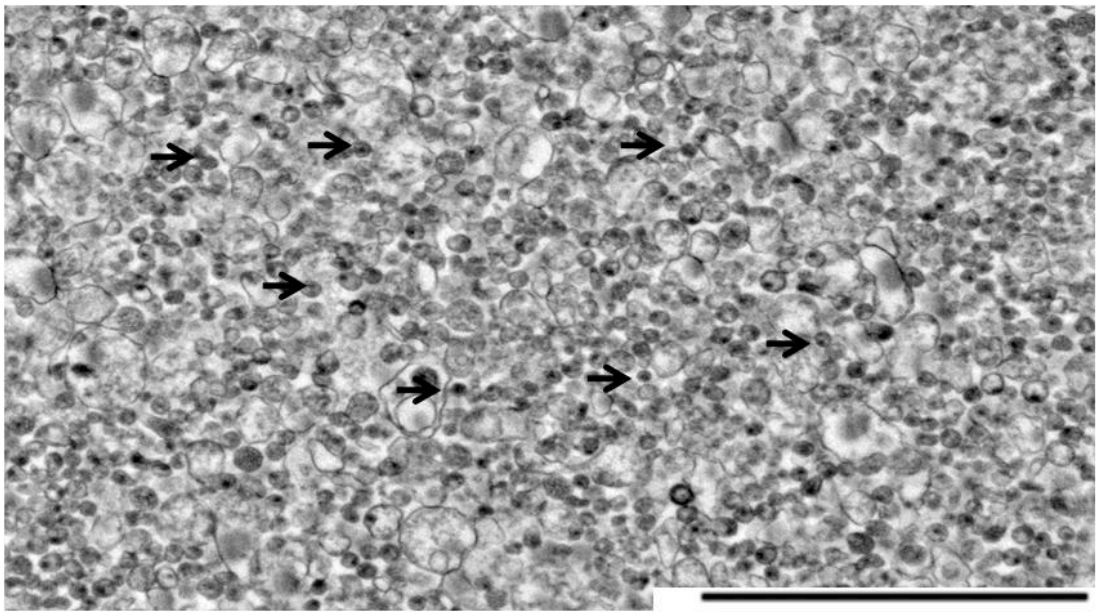

b

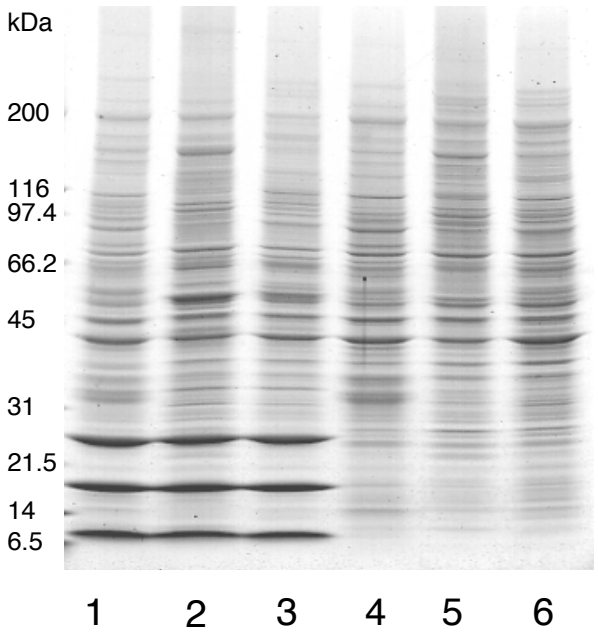

c

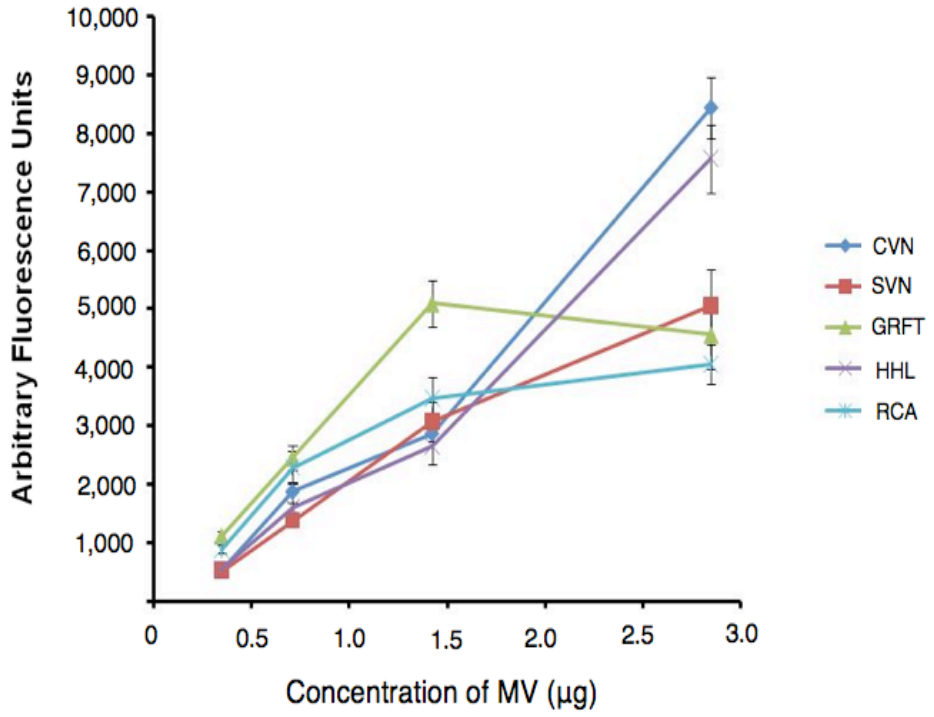
Arbitrary Fluorescence Units
10,000
9,000
8,000
7,000
6,000
5,000
4,000
3,000
2,000
1,000
0
0.5
1.0
1.5
2.0
2.5
3.0
Concentration of MV (µg)
CVN
SVN
GRFT
HHL
RCA

d

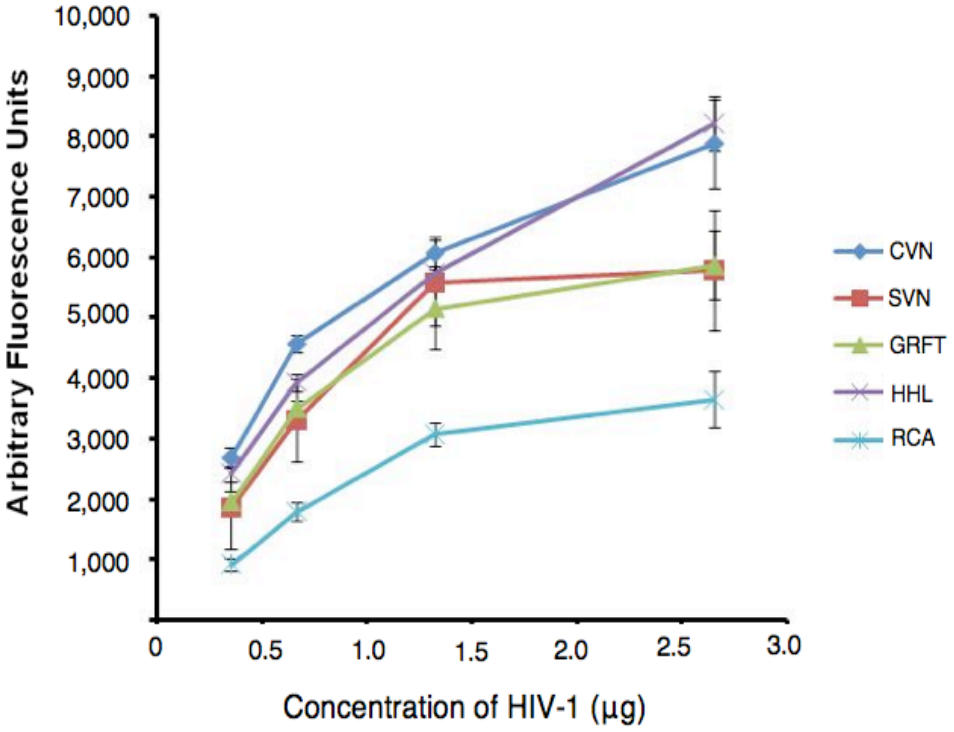
Arbitrary Fluorescence Units
10,000
9,000
8,000
7,000
6,000
5,000
4,000
3,000
2,000
1,000
0
0.5
1.0
1.5
2.0
2.5
3.0
Concentration of HIV-1 (µg)
CVN
SVN
GRFT
HHL
RCA

e

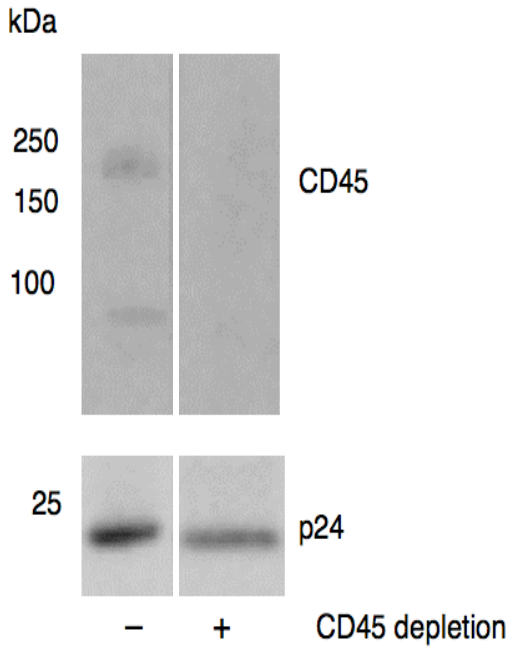

Supplementary Figure 2. Evidence for the viral purity of H9-derived HIV samples. (**a**) Electron microscopic analysis of HIV-1 virions isolated from H9 cells The scale bar represents 2 microns and arrows identify examples of virions in the preparations. (**b**) SDS-PAGE analysis of microvesicles and HIV-1 from 3 T-cell lines (H9, SuptT1 and Jurkat-Tat-CCR5). 100 μg of protein sample was loaded per lane and the gel was stained with Gelcode blue. The lanes are as follows: 1. HIV-1(MN) CL.4/ H9 2. HIV-1(MN) CL.4/SupT1 3. HIV-1(MN) /Jurkat-Tat-CCR5 4. H9 MV 5. SupT1 MV 6. Jurkat-Tat-CCR5 MV. (**c-d**) Dose response of labeled MV and HIV samples on the lectin microarray. Lectin microarrays were hybridized with different amounts of Cy3-labeled (**c**) H9-derived MV or (**d**) H9-derived HIV. The dose-response curves of select lectins are shown as a function of the average median fluorescence based on 5 spots per array. The bars represent the standard deviation. Given that our arrays are

typically hybridized with ~1 μg of sample per array this data confirms that, for the majority of lectins, our data is in the linear signal range. This data disproves the notion that a 5-fold dilution of glycans would not be observed, as would be the case if MV contamination of HIV-1 were responsible for the signal on our arrays. (**e**) Western blot analysis confirms the presence of the viral capsid protein (p24) in both CD45 immunodepleted and undepleted HIV samples derived from H9 cells and the absence of CD45.

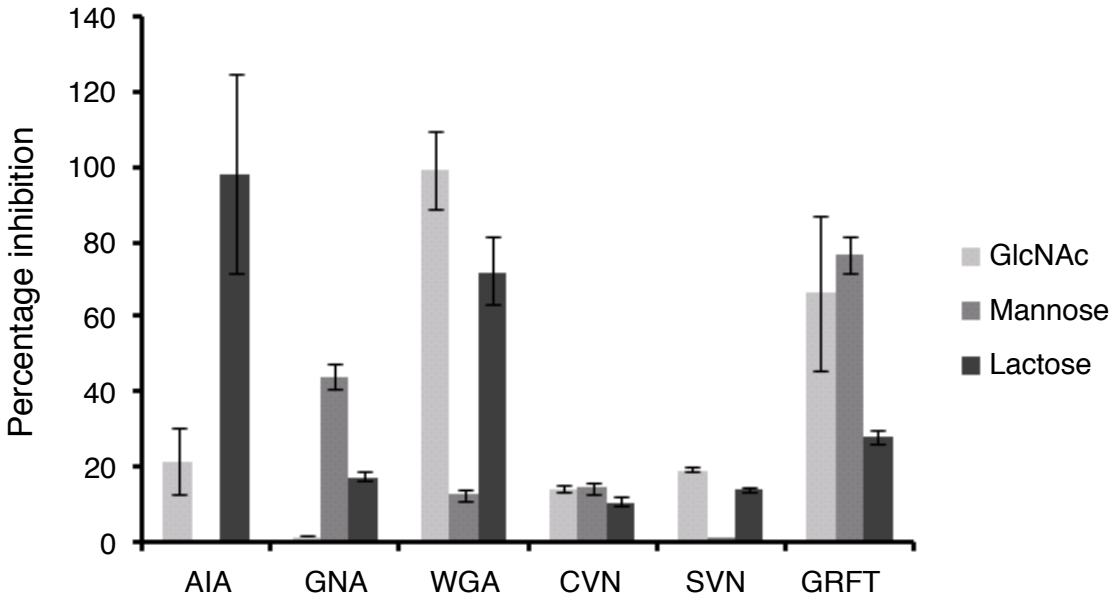

Supplementary Figure 3. Inhibition with small panel of carbohydrates confirms that the interactions are carbohydrate based. Lectin microarrays were preincubated with the appropriate carbohydrates (*N*-acetylglucosamine,GlcNAc, **5**, light grey; lactose, **4**, medium grey; mannose, **3**, dark grey) or buffer (control), followed by addition of Cy3-labeled H9-derived HIV samples. The inhibition profile for a representative subset of lectins is shown. The graph depicts the % inhibition of each lectin which was calculated as follows: 100 * ((Average median fluorescence intensity control - Average median fluorescence intensity carbohydrate inhibited array) /(Average median fluorescence intensity control)) = % inhibition. The errors were propagated using the standard deviations and standard propagation of error equations. Inhibition experiments were also performed with both membrane preparations and microvesicles (data not shown).

a

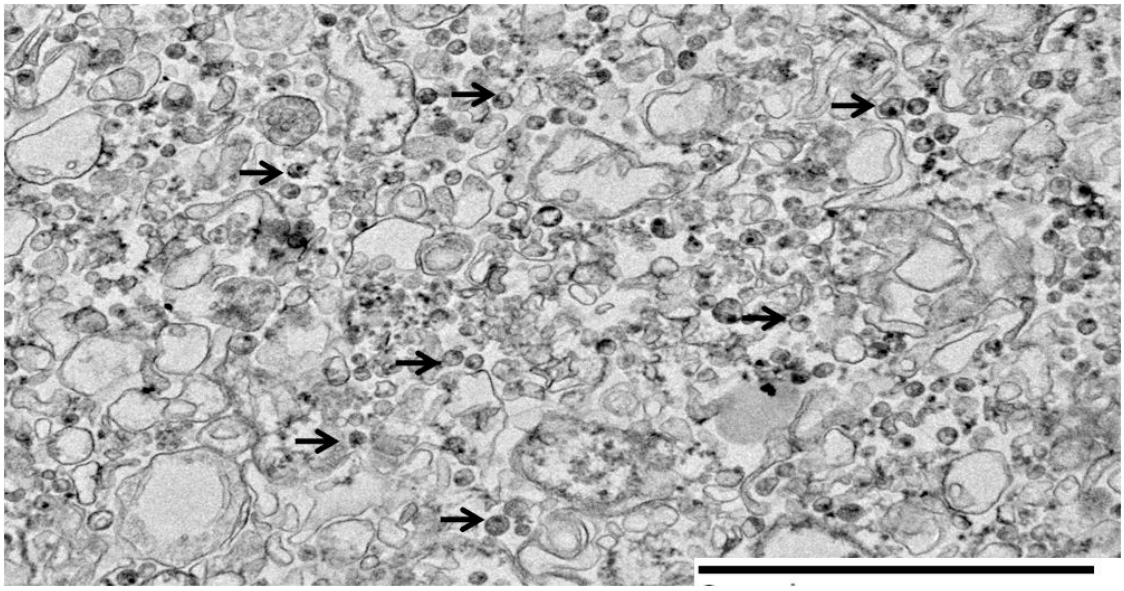

b

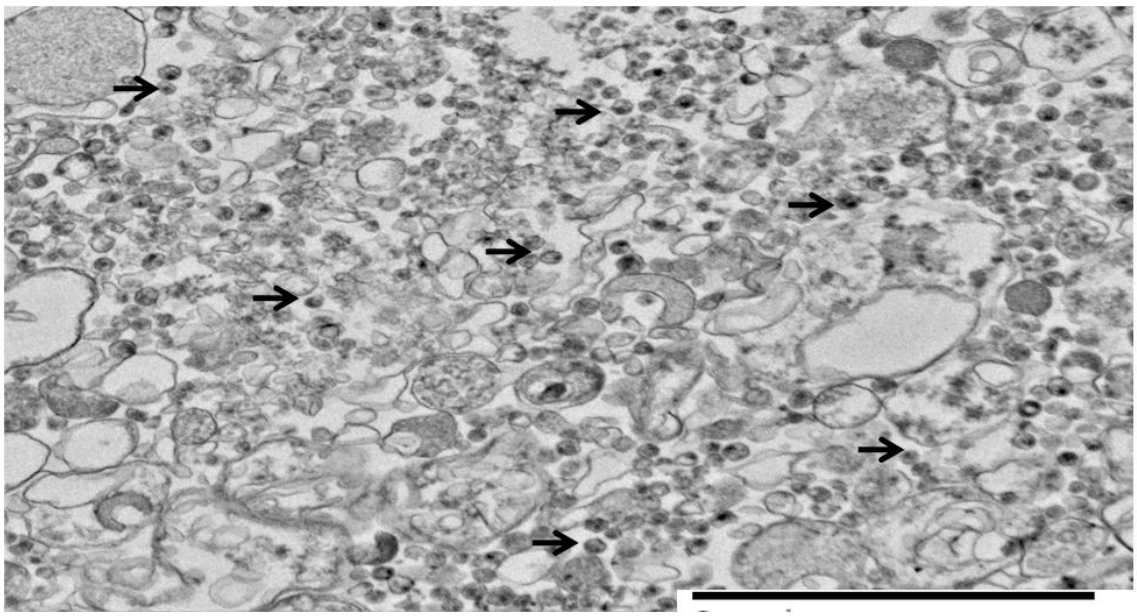

Supplementary Figure 4. Electron micrographs of representative SupT1 and Jurkat-Tat-CCR5 HIV viral preparations. Electron microscopic analysis of HIV-1 virions isolated from (**a**) SupT1 cells and (**b**) Jurkat-Tat-CCR5 cells. The scale bar represents 2 microns and arrows identify examples of virions in the preparations.

a

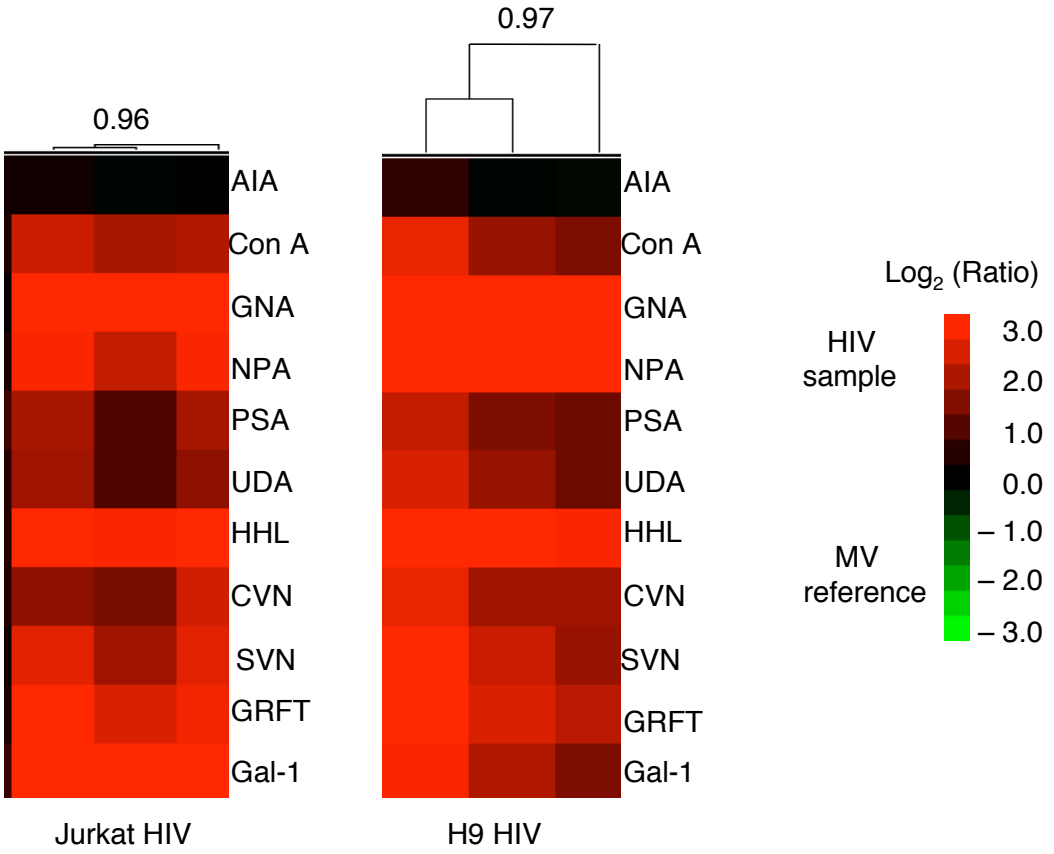

b.

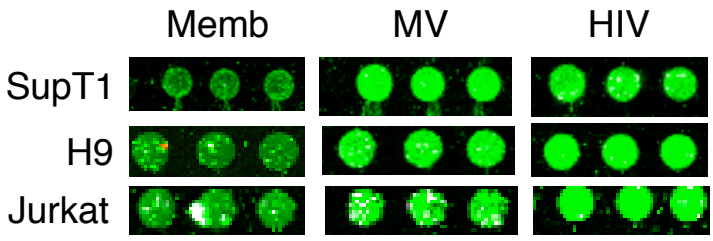

Supplementary Figure 5. Binding of mannose specific lectins to HIV and microvesicles. (**a**) To facilitate direct comparison of HIV and microvesicles, equal amounts of H9- and Jurkat-Tat-CCR5-derived HIV samples (1 μg) were hybridized against microvesicles derived from their respective uninfected cells

(1 μg, biological reference), with two arrays (dye-swapped pair) run for each sample to generate Yang correlations as before. The hierarchical cluster map of a select group of mannose-binding lectins is shown. AIA, which binds *N*-acetyl galactosamine residues, is shown as a control. Red indicates enhanced binding to the sample while green indicates enhanced binding to the microvesicles. HIV clearly shows 4-8-fold better binding to mannose lectins than the matched microvesicles in both cell lines. (**b**) MV and HIV derived from all three T-cell lines show increased affinity to the high mannose binding lectin cyanovirin (CVN) when compared to their respective cell membrane samples. This is representative of the relative binding to lectins recognizing high mannose in our panel and illustrates that although mannose-binding lectins bind more strongly to HIV, they still have strong binding to the microvesicles as well.

a

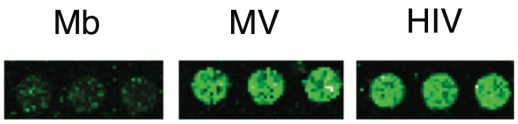

b

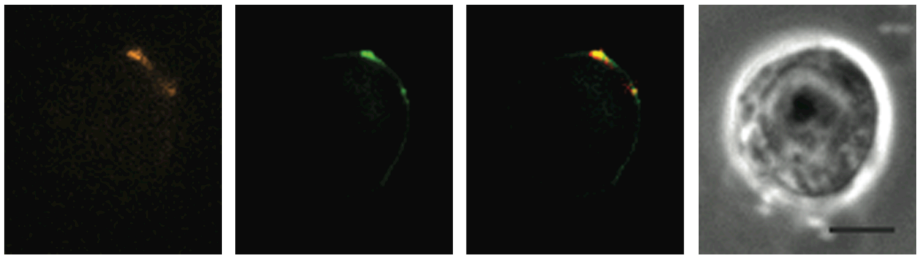

c

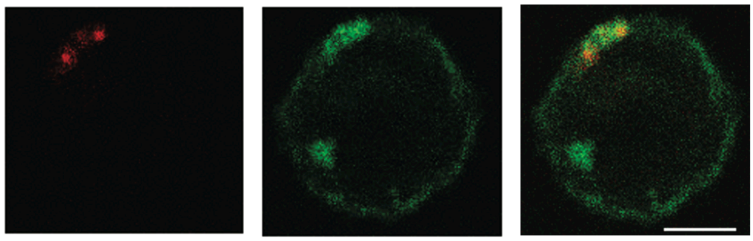

Supplementary Figure 6. Glycan epitopes enriched in microvesicles and HIV-1 localize to specific domains of the plasma membrane. N-Rh-PE enriched domains co-localize with select FITC-labeled lectins on Jurkat-Tat-CCR5 (Jurkat) cell surfaces. (**a**) MV and HIV-1 from Jurkat cells exhibit increased binding to PHA-L in comparison to the Jurkat cell membrane (Mb). (**b**) Jurkat cells were labelled with N-Rh-PE, fixed, stained with FITC-PHA-L and

examined using fluorescence microscopy. N-Rh-PE domains (red) colocalize with domains that are enriched in glycans recognized by PHA-L (green). (**c**) Cells stained with FITC-DSA and N-Rh-PE were examined using confocal microscopy. As expected, cell surface domains enriched in N-Rh-PE staining (red) colocalized with FITC-DSA (green). A representative image is shown. Colocalization was observed at the cell surface throughout the z-axis image planes.

a

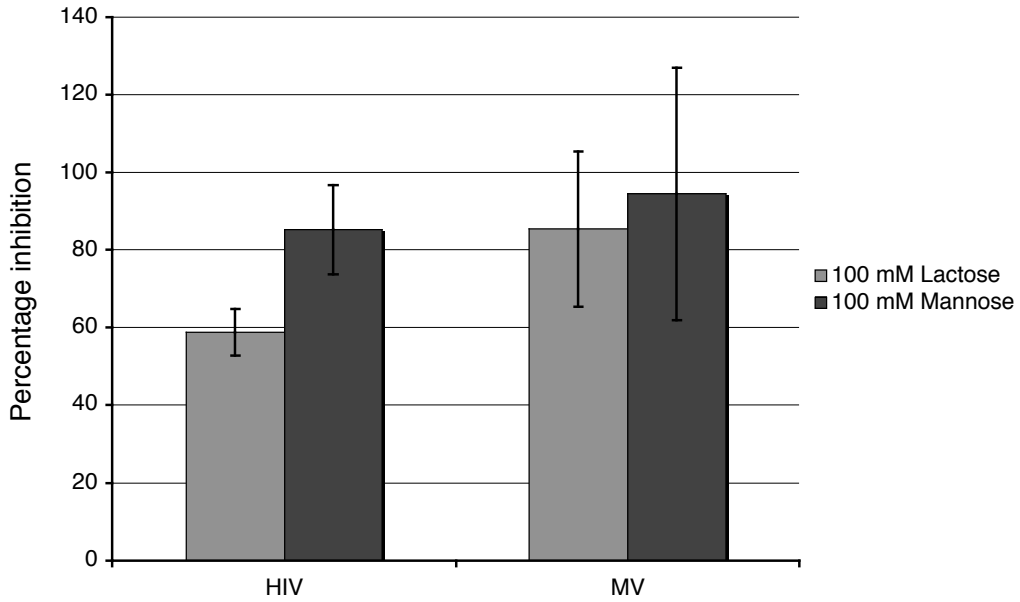

b.

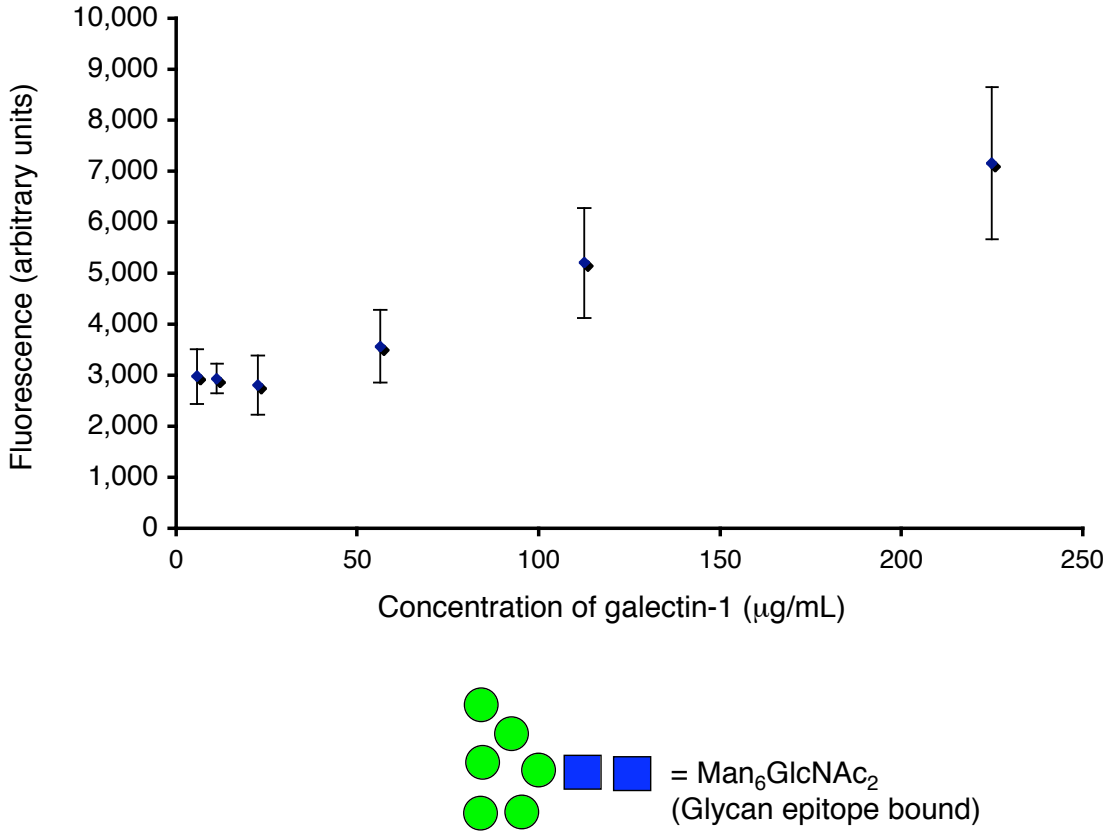

= $Man_6GlcNAc_2$
(Glycan epitope bound)

Supplementary Figure 7. Lactose inhibition of microvesicles and examination of the Consortium for Functional Glycomics data for galectin-

1. a) In contrast to mannose, which causes >85% inhibition of galectin-1 binding to both H9-derived MV and HIV-1, lactose inhibits HIV-1/galectin-1 interactions only 59%, but inhibits the MV signal 85%. This data shows that galectin-1 is active on the array and displays lactose dependent binding as previously reported [1]. However, the inability of lactose to inhibit galectin-1 binding to HIV-1 argues that interactions with the virus may be through a different binding motif, most likely clustered high mannose. Lectin microarrays were preincubated with 200 mM of the appropriate carbohydrate (lactose ,medium grey or mannose, dark grey) for 30 min, followed by addition of Cy3-labeled H9-derived HIV or MV samples. The graph depicts the % inhibition of each lectin, which was calculated as shown in Supplementary Fig. 5. Errors were propagated using the standard deviations and standard propagation of error equations. b) Using publicly available data on galectin-1 binding to carbohydrate microarrays from the Consortium for Functional Glycomics, which has been utilized in a publication[1], we graphed the dose-dependent binding of galectin-1 to a high mannose epitope present on their carbohydrate microarray (Glycan 197, $Man_6GlcNAc_2$). The average fluorescence without the minimum and maximum spots is shown vs. the concentration of galectin-1 (μg/mL). The error bars represent the standard deviation. This epitope was seen to improve as a relative binder as the concentration of galectin-1 decreased. Despite the presence of other high mannose epitopes on the array, this ligand was the only high mannose ligand that presented a consistent positive signal in this set of assays. However, at some concentrations, this ligand bound galectin-1 with a signal comparable to or higher than LacNAc epitopes (Glycans 152 and 153,

data not shown). This implies that some high mannose epitopes may indeed be ligands for galectin-1.

Supplementary Table 1. Lectin panel for microarray.‡

Lectin	Abbreviation	[Print] (μg/mL)	Print Sugar	Rough Specificity*
Abrus precatorius	APA	500	Gal	Gal β-1,3GalNAc (TF antigen) > Gal,
Agaricus bisporus	ABA	500	Gal	Gal β-1-3GalNAc
Aleuria aurantia	AAL	1000	Fuc	Fuc
Anguilla anguilla	AAA	1000	Fuc	α-Fuc
Arachis hyogaea	PNA	500	Gal	Terminal Gal β-OR
Artocarpus intergrifolia (Jacalin)	AIA	500	Gal	α-GalNAc not substituted at C-6 (i.e. core 1, 3, T-antigen but not core 2).
Bauhinia purpurea	BPA	500	Gal	Primarily Gal β-1,3 or 1,4 but will also bind β-GalNAc more weakly
Black bean crude	Blackbean	1000	Lac	GalNAc
Bryonia dioica	BDA	500	Gal	GalNAc
Canavalia ensiformis	Con A	500	Man	branched and terminal mannose, terminal GlcNAc
Cancer antennarius	CCA	500	Lac	9-*O*-Acetyl Sia and 4-*O*-Acetyl Sia
Caragana arborescens	CAA	500	Gal	GalNAc/Gal (monosaccharides best)
Cicer arietinum	CPA	1000	Lac	Complex
Colchicum autumnale	CA	500	Gal	Terminal Gal β-OR
Cystisus scoparius	CSA	500	Gal	β-GalNAc, terminal
Cyanovirin	CVN	500	Man	α-1,2 mannose
Datura stramonium	DSA	500	Lac	GlcNAcβ-1,4GlcNAc oligomers and LacNAc
Dolichos biflorus	DBA	500	Gal	GalNAcα-OR
Erythrina cristagalli	ECA	1000	Gal	LacNAc and GalNAc
Euonymus eurpaeus	EEA	1000	Lac	Blood Groups B and H
Galanthus nivalis	GNA	500	Man	terminal α-1,3 mannose
Galectin-1	Gal-1	2500	Lac	LacNAc
Glycine max	SBA	500	Gal	terminal GalNAc
Griffithsin	GRFT	1000	GlcNAc	Mannose, GlcNAc
Griffonia simplicifolia I	GS-I	500	Gal	α-galactose
Griffonia simplicifolia II	GS-II	500	GlcNAc	terminal GlcNAc
Helix pomatia	HPA	500	Gal	α-GalNAc terminal
Hippeastrum Hybrid	HHL	1000	Man	α-1,3 mannose and α-1,6 mannose
Homaris americanus	HMA	500	Lac	sialic acid
Iberis Amara	IAA	500	Lac	GalNAc
Laburnum alpinum	LAA	500	GlcNAc	GlcNAc oligomers
Lens culinaris	LcH	1000	Man	Complex (Man/GlcNAc core with α-1,6 Fuc)
Limax flavus	LFA	500	Lac	α-Sia

Limulus polphemus	LPA	500	Lac	α-Sia
Lotus tetragonolobus	LTL	500	Fuc	Terminal α-Fuc, Le^x
Lypersicon esculentum	LEA	1000	GlcNAc	β-1,4GlcNAc oligomers
Maackia amurensis	MAL-I	1000	Lac	LacNAc
Maackia amurensis	MAL-II	1000	Lac	α-2,3 sialic acid
Maackia amurensis	MAA	500	Lac	α-2,3 sialic acid
Narcissus pseudonarcissus	NPA	1000	Man	Terminal and internal Man
Persea Americana	PAA	500	GlcNAc	Unknown
Phaseolus lunatus	LBA	1000	Gal	GalNAcα-1,3[Fucα-1,2]Gal
Phaseolus vulgaris-L	PHA-E	500	Lac	complex
Phaseolus vulgaris-L	PHA-L	500	Gal	β-1,6 branched trimannosyl core N-linked glycans
Pisum sativum	PSA	1000	Man	Man
Polyporus Squamosus	PSL	500	Lac	α-2,6 sialic acid
Psophocarpus tetragonolobus	PTA	500	Gal	Gal
Psophocarpus tetragonolobus	PTL-I	1000	Gal	α-GalNAc
Psophocarpus tetragonolobus	PTL-II	1000	Gal	α-1,2 fucosylated LacNAc
Ricin B chain	RCA	1000	Lac	β-Gal/GalNAc
Robinia pseudoacacia	RPA	1000	Lac	Complex
Sambucus nigra	SNA	500	Lac	α-2,6 sialic acid on LacNAc
Scytovirin	SVN	500	Man	α-1,2 mannose
Solanus tuberosum	STA	500	GlcNAc	GlcNAc oligomers, LacNAc
Sophora japonica	SJA	1000	Gal	GalNAc
Trichosanthes kirilowii	TKA	500	Gal	β-Gal, LacNAc but Sia-α-2,3 or 2,6 inhibits best.
Trifolium repens	RTA	500	GlcNAc	2-deoxy-Glu
Tritiicum vulgare	WGA	1000	GlcNAc	β-GlcNAc, sialic acid, GalNAc
Tulipa sp.	TL	1000	GlcNAc	GlcNAc
Ulex europaaeus I	UEA-I	500	Fuc	α-1,2 fucose on LacNAc
Ulex europaaeus II	UEA-II	500	GlcNAc	GlcNAc oligomers
Uritica dioica	UDA	500	GlcNAc	GlcNAc β-1,4GlcNAc oligomers and high mannose epitopes
Vicia fava	VFA	500	Gal	Man>Glc>GlcNAc
Vicia graminea	VGA	500	Gal	O-linked Gal β-1,3GalNAc clusters
Vicia villosa	VVA	500	Gal	GalNAc
Vicia villosa	VVA (man)	500	Gal	Man
Vigna radiata	VRA	500	Gal	α-Gal
Wisteria floribunda	WFA	500	Gal	GalNAc

‡*Abbreviations:* Glu (Glucose), Gal (Galactose), GlcNAc (*N*-acetyl-D-glucosamine), GalNAc (*N*-acetyl-D-galactosamine), Man (Mannose), Fuc (Fucose), Sia (Sialic Acid), Lac (Lactose), LacNAc (*N*-acetyl-D-lactosamine), Le^x (Lewis x antigen).

*Specificity data was compiled from a variety of sources including the Consortium for Functional Glycomics Carbohydrate Array Analysis (http://www.functionalglycomics.org/glycomics/publicdata/primaryscreen.jsp) and the Handbook of Plant Lectins (1998, Wiley and Sons).

Supplementary Table 2. Cell lines, Microvesicles and HIV-1 used in this study.

Agent	Cell Line Number	Replicate	Product Lot
H9 MV	CLN283	1	P4075
		2	P4076
		3	P4077
HIV-1(MN) CL.4/ H9	CLN71	1	P3935
		2	P3945
		3	P3944
HIV-1(MN) CL.4/SUPT1	CLN219	1	P4095
		2	P4092
		3	P4098
SUPT1 MV	CLN52	1	P3772
SIVmac-NC/SUPT1	CLN130	1	P3700
SIVmac-CP/SUPT1	CLN131	1	P3866
HIV-1(MN)/Jurkat-Tat-CCR5	CLN284	1	P4066
		2	P4067
		3	P4068
Jurkat-Tat-CCR5 MV	CLN259	1	P4058
		2	P4060
		3	P4061

Supplementary methods

Microarray Data Analysis. For the cluster analysis, only lectins passing our quality control measurement [2], as determined by glycoprotein standards, that were "positive" for one or more samples were used. "Positive" lectins were determined using single color data for each sample as follows. For each lectin in a sample, the median fluorescence signal intensity of each spot was divided by the local median background to give a signal to noise ratio (S/N). The S/N of the 5 replicate spots per lectin were tested for significant outliers using Grubbs' outlier test. If a significant outlier was found, it was discarded and the remaining values were averaged. Only lectins where the S/N + 1 standard deviation was greater than or equal to 5 were considered positive.

For dual-color analysis, we tested the background-subtracted median fluorescence signal intensities for each lectin in each channel for significant outliers using Grubbs' outlier test (n=5 spots). Significant outliers were discarded and the average of these tested values was used to calculate the Yang correlation values [3] using the data from two orthogonally labeled sample sets (i.e. two arrays) for each lectin on the array (Yang correlation = $((\text{Log}_2 (\text{Sample A}_{\text{Cy3}} \div \text{Biological Reference}_{\text{Cy5}}) + \text{Log}_2 (\text{Sample A}_{\text{Cy5}} \div \text{Biological Reference}_{\text{Cy3}}) \div 2)$). We created the hierarchical clustering maps using Cluster 3.0 with Java Treeview (http://rana.lbl.gov/EisenSoftware.htm) [4]. Unless otherwise indicated, the Pearson correlation coefficient was used as the distance metric for the samples with average linkage analysis. P-value calculations (two-tailed) were done using the Student t determination on the

website http://faculty.vassar.edu/lowry/tabs.html#r with n-2 for the degrees of freedom.

CD45 immunodepletion of HIV-1 virions. Fluorescently labelled H9 derived HIV-1 virions were immunodepleted using anti-CD45-conjugated paramagnetic microbeads (Miltenyi Biotech, Auburn, CA) as previously described [5].

Western blot analysis. Equal amounts of CD45 immunodepleted and non-depleted virus samples were analyzed by SDS-PAGE and transferred to a nitrocellulose membrane. The membrane was blocked for 1 h in block buffer (5% BSA in TBS, 0.1% Tween) and then incubated with either anti-p24 antibody (1:50,000, AIDS Vaccine Research Program, NCI) or anti-CD45 antibody (1:500, Clone 69, BD Transduction Laboratories, San Jose, CA) in blocking buffer for 1 h. The membrane was then washed (6 x with TBST) and incubated with goat-anti-mouse-HRP (1:10,000, BioRad, Hercules, CA) for 1 h. The membrane was then rinsed 6 x with TBST and visualized using chemiluminescent substrate (West Femto substrate, Pierce, Rockford, IL).

Electron microscopy [6]. The HIV pellet was prepared for electron microscopy analysis by adding equal volumes of fixative (2% glutaraldehyde in 0.1 M sodium cacodylate) and centrifuged at 60,000 rpm for 6 minutes at 4ºC. The supernatant was discarded and the pellet was overlaid with fixative. The sample was further processed as described previously and examined, imaged by Hitachi 7600 microscope operated at 80kV.

Fluorescence microscopy of PNGase F-treated Jurkat cells. Jurkat-Tat-CCR5 cells were adhered to poly-Lysine coated glass bottom dishes and fixed as described above. We then treated the fixed cells with 100 U of PNGase F (New England Biolabs, Ipswich, ME) in PBS or PBS alone at 37 °C for 1 h. Cells were washed with PBS (3 × 5 min) and stained with FITC-conjugated DSA. We obtained fluorescence images as described previously.

Confocal Microscopy. For confocal microscopy, cells were prepared as previously described. Confocal images were obtained using the Leica confocal system TCS4D with a 63x oil immersion lens (NA 1.4; FITC: ex. 503 nm, em. 552 nm; Rhodamine: ex. 561 nm, em. 624 nm; Core Facility, Institute for Cell and Molecular Biology, University of Texas, Austin, TX).

Inhibition experiments. We preincubated our lectin microarrays with either 200 mM (50 mL in PBS) of the appropriate carbohydrate (mannose and lactose) or buffer (control) for 30 min prior to the addition of Cy3-labeled H9-derived HIV samples (1 mg, 50 mL in PBS with 0.1 % Tween) for a final concentration of 100 mM inhibitory sugar. Samples were incubated for 2 h and slides were processed as before.

References

1. Stowell, S. R. et al. Galectins-1, -2 and -3 exhibit differential recognition of sialylated glycans and blood group antigens. J Biol Chem (2008).

2. Pilobello, K.T., Slawek, D.E. & Mahal, L.K. A ratiometric lectin microarray approach to analysis of the dynamic mammalian glycome. *Proc. Natl. Acad. Sci. U. S. A.* **104**, 11534-11539 (2007).

3. Yang, Y.H. *et al.* Normalization for cDNA microarray data: a robust composite method addressing single and multiple slide systematic variation. *Nucleic Acids Res.* **30**, e15 (2002).
4. Eisen, M.B., Spellman, P.T., Brown, P.O. & Botstein, D. Cluster analysis and display of genome-wide expression patterns. *Proc. Natl. Acad. Sci. U. S. A.* **95**, 14863-14868 (1998).
5. Trubey, C.M. *et al.* Quantitation of HLA class II protein incorporated into human immunodeficiency type 1 virions purified by anti-CD45 immunoaffinity depletion of microvesicles. *J. Virol.* **77**, 12699-12709 (2003).
6. Mariner, J. M., McMahon, J. B., O'Keefe, B. R., Nagashima, K. & Boyd, M. R. The HIV-inactivating protein, cyanovirin-N, does not block gp120-mediated virus-to-cell binding. Biochem Biophys Res Commun 248, 841-5 (1998).